

UNCLASSIFIED

AD 411167

DEFENSE DOCUMENTATION CENTER

FOR

SCIENTIFIC AND TECHNICAL INFORMATION

CAMERON STATION, ALEXANDRIA, VIRGINIA



UNCLASSIFIED

DISCLAIMER NOTICE

THIS DOCUMENT IS BEST QUALITY PRACTICABLE. THE COPY FURNISHED TO DTIC CONTAINED A SIGNIFICANT NUMBER OF PAGES WHICH DO NOT REPRODUCE LEGIBLY.

NOTICE: When government or other drawings, specifications or other data are used for any purpose other than in connection with a definitely related government procurement operation, the U. S. Government thereby incurs no responsibility, nor any obligation whatsoever; and the fact that the Government may have formulated, furnished, or in any way supplied the said drawings, specifications, or other data is not to be regarded by implication or otherwise as in any manner licensing the holder or any other person or corporation, or conveying any rights or permission to manufacture, use or sell any patented invention that may in any way be related thereto.

ABSTRACT

The cathodic polarization behavior of NiSi, NiAs, NiSb, NiTe₂, and NiS at room temperature ~~has been~~ determined in 1 M perchlorate solutions at pH 0.04 and pH 10.8 up to -1.0 volts vs. R. H. E. Measurements were also made on Ni, Si, Sb, Te, and on Ni electrodes exposed to As₂O₃ and H₂S. Sb, Te, Si and Ni/As₂O₃ exhibit kinetic peculiarities which are probably attributable to hydride formation, but these features are not generally shown by the corresponding nickel compounds. With the exception of Si in acid solution, all of the electrodes show an extended Tafel line indicating the hydrogen evolution reaction, ~~with the following parameters:~~

	pH 0.04		pH 10.8	
	b (mV)	-log i ₀ (A/cm ²)	b (mV)	-log i ₀ (A/cm ²)
Ni	125	5.3	105	5.0
Ni + As ₂ O ₃	120	8.0	no effect on Ni	
NiAs	56	7.3	155	6.1
Si	no Tafel region		168	7.5
NiSi	113	5.4	145	5.4
Sb	170	5.7	260	5.3
NiSb	108	7.6	245	5.0
Te	48	11	-	-
NiTe ₂	55	8	-	-
Ni/H ₂ S	80	9.4	no effect on Ni	
NiS	62	7.2	100	4.9

For NiAs, NiTe₂, and NiSi, there exist regions where the current densities at a given overpotential exceed those on either of the individual elements. The results are discussed with a view to distinguishing the role of atomic and crystal factors in the electrocatalytic activity of the electrode materials. The intrinsic chemical properties of the surface atoms appear to dominate the mechanism of the h. e. r., while the crystalline properties strongly influence the rates.

I. INTRODUCTION

Two general approximations are useful in interpreting the chemical activity of crystalline surfaces. The first, which may be designated the "atomic approach", cites the intrinsic reactivity of the individual surface atoms, and treats the crystal environment as a perturbation. This approach has been effective, for instance, in treating the chemisorption of oxygen on metalloid surfaces⁽¹⁾, the dissolution reactions of compound semiconductors⁽²⁾, and the excess reactivity of line dislocations⁽³⁾. The alternative approach concentrates on the structural and electronic properties of the crystal as a whole, and attaches but secondary significance to the specific atomic composition. Advocates of this "crystal approach" point, for example, to chemisorption and catalysis on transition metal alloys⁽⁴⁾ and on semiconducting oxides⁽⁵⁾.

In electrochemical surface reactions evidence can be found to support both views. Thus, the rates of redox reactions such as the ferrous/ferric ion reaction at mercury and platinum surfaces⁽⁶⁾ are determined by the electronic properties of the electrode as a whole. On the other hand, the passivation of titanium by trace additions of platinum⁽⁷⁾ seems to imply that hydrogen discharge is an intrinsic property of the platinum atoms themselves. A particularly interesting case is the anodic dissolution of germanium. At low current densities, the course of reaction is strongly conditioned by the chemical properties of the surface atoms, while at high current densities, the rate is limited by what is unambiguously a crystal property, viz., the diffusion of electron holes to the reacting interface⁽⁸⁾.

The distinction between the atomic and crystal factors is of heuristic value in studies of surface reactivity. Either approximation provides a point of departure for elaborating the details of mechanism, and, at the same time, comprises an immediately useful guideline for optimizing the properties of new technical materials.

The objective of the present series of studies is to clarify the influence of crystal environment upon the electrochemical, and particularly the electrocatalytic, properties of a transition metal atom. We have chosen to examine several compounds of nickel with elements from Groups IVB, VB, and VIB of the Periodic Table. The use of such compounds was

avored for two reasons: the clear chemical differences between the component elements, and the highly ordered atomic coordination.

Each of the compounds is a semi-metal whose cohesive energy is concentrated in large part among directed covalent bonds between nickel and its companion element. Direct cation-cation valencies are also present, however, and are evidenced by the various crystal structures⁽⁹⁾. For example, NiAs and NiSb both take on the $B8_1$ structure in which the nickel sublattice exhibits simple hexagonal symmetry, while the interpenetrating As or Sb sublattice exhibits close-packed hexagonal packing. If direct interactions between the nickel atoms were absent, the c/a ratio of the crystals would equal 1.33 in consequence of the anion sublattice. Actually, $c/a = 1.390$ for NiAs and 1.308 for NiSb, the distortion being attributable to direct cation-cation interaction in the c -direction⁽¹⁰⁾.

In the present paper, we describe the cathodic polarization characteristics of NiSi, NiAs, NiSb, NiS, and NiTe₂ electrodes and compare the results with those obtained on their constituent elements. The elements have been studied in the form of bulk crystals (Ni, Sb, Si, and Te) or as adsorbed films on nickel (As). Special emphasis is placed upon electrocatalysis of the hydrogen evolution reaction (h. e. r.).

II. EXPERIMENTAL PROCEDURES

The compounds were prepared from spectroscopically pure elements by direct fusion of stoichiometric mixtures in evacuated quartz capsules, directional freezing from the melt, and annealing just below the melting points. The melting points and relevant phase diagrams are given by Hansen⁽¹¹⁾. The ingots were all obtained as single phase material; the NiAs, NiSb, and the NiTe₂ consisted of several large crystal grains, while the NiS and NiSi were dense but microcrystalline. The elemental Ni, Sb, Si and Te samples all consisted of single crystal sections. The silicon sample was semiconductor grade material doped with 1 p. p. m. of phosphorus, which imparts an electrical conductivity of $1 (\Omega\text{-cm})^{-1}$.

Cylindrical specimens were cut from each sample and mounted in a close-fitting Pyrex holder with Kel-F wax⁽¹²⁾. Flat surfaces with a geometric area of $\sim 0.75 \text{ cm}^2$ were exposed by grinding, followed by

mechanical polishing, and, where possible, by chemical or electrolytic polishing. The samples were then washed ultrasonically, treated with chromic acid/sulfuric acid cleaning solution, thoroughly rinsed with triply distilled water, and transferred directly to the test cell.

An all-Pyrex three-compartment cell was employed in which the working electrode was separated from a platinum counter electrode by a glass frit. The solutions employed were 1 M perchloric acid (pH = 0.04) and 1 M sodium perchlorate adjusted to pH = 10.8. Potentials were measured against a reversible hydrogen electrode in the same solution. Potentiostatic and, occasionally, galvanostatic methods were used to obtain steady-state polarization data. The solutions were stirred by a stream of hydrogen or nitrogen which was purified by passage through a liquid nitrogen trap.

The electrode under study was transferred to the test solution and was immediately polarized stepwise to potentials negative to the reference hydrogen electrode in the same solution. When the cathodic current exceeded 0.3 A/cm^2 or the potential exceeded -1.0 V , the path was retraced to the rest potential (in galvanostatic measurements), or until the direction of the current was reversed by the onset of anodic dissolution (in potentiostatic measurements).

III. RESULTS

The results are summarized in Figs. 1-6 as plots of potential vs. logarithm of the current density. All potentials are referred to the standard hydrogen electrode; the current densities (C. D.) are in amperes per unit geometric area of the electrode surface. In each Figure, the results for elemental nickel are given for ready comparison. The dispersion in the nickel data, shown in detail in Fig. 1, covers the results for about ten independent experiments in which the effects of remounting the electrode, of mechanical vs. electrochemical polishing, of extended preelectrolysis, and of recycling were observed. The degree of reproducibility and the absolute values of the data on nickel compare favorably with other work⁽¹³⁾. Included in the bands of data are slight hysteresis effects, i. e., higher overpotentials in the direction of decreasing current than in the opposite direction.

Virtually all of the results show a positive deviation from the Tafel line at C. D. 's exceeding 10^{-2} A/cm². Since the deviation depends upon current rather than potential, it is unlikely to result from a fundamental effect, such as increasing surface coverage by hydrogen atoms. It is more probably an artifact due to partial blocking of the surface by hydrogen bubbles generated by the h. e. r.

NiSi and Si

Fig. 2 summarizes the results for Ni, Si, and NiSi, in both acid and alkaline solutions. Elemental silicon shows a complex behavior, probably attributable to the effects of SiO₂ which is stable throughout the potential range under study. ($\text{SiO}_2 + 4\text{H}^+ + 4\text{e} = \text{Si} + 2\text{H}_2\text{O}$; $E_o = -0.86 \text{ V}$)* (14). In the direction of increasing overpotential the polarization curve shows a sharp upswing at currents exceeding $\sim 0.5 \text{ mA/cm}^2$. In this region, the variation of current at constant potential showed a curious time dependence. The current decreased, e. g., from 1.2 mA/cm^2 to 0.4 mA/cm^2 at 0.5 V, then jumped back to the original value from whence it repeated the decay with a frequency of about 1 cycle/2 min. The apparent decrease in the cathodic current may result from an increase in oxide thickness by the slow anodic oxidation which occurs even at negative potentials. Under the conditions of the experiment the surface appears unchanged; the absence of interference colors implies a total oxide thickness $< 1000 \text{ \AA}$. The rapid jump to higher cathodic currents implies mechanical breakdown of the oxide when the thickness exceeds a critical value. The total anodic current must be smaller than that corresponding to the predominant cathodic reaction, which is doubtlessly hydrogen evolution. Further evidence for anodic film formation comes in the return to lower potentials after a prolonged period at -700 mV. During the return there is no longer evidence for the cyclic growth and breakdown, but as the potential is adjusted to values below -300 mV, a pronounced anodic transient is observed before the cathodic current takes over.

* The Stockholm Sign Convention is followed.

In the direction of decreasing overpotential the current decreases linearly with potential. The apparent ohmic resistance is $1200 \Omega\text{-cm}^2$; assuming an average film thickness of 100 \AA in this potential region, one obtains a resistivity $\rho \sim 10^9 \Omega\text{-cm}$, which is not unreasonable for SiO_2 . It is probable, therefore, that the characteristics of the cathodic polarization curve on Si in acid solutions are determined primarily by the oxide film. A similar conclusion was reached by Turner⁽¹⁵⁾.

The results on Si in alkaline solution bear a superficial resemblance to those in acid solution. One important distinction is the direct dependence of the current upon stirring in the region of sharply rising overpotential. This implies that the rate is limited by a diffusion process in the region of the electrode-electrolyte interface. We tentatively suggest that the current in this region is not due to h. e. r., but to the direct reduction of Si to SiH_4 , ($\text{Si} + 4\text{H}_2\text{O} + 4 e = \text{SiH}_4 + 4 \text{OH}^-$; E_0 (pH 10.8) = 0.541 V)⁽¹⁶⁾. This reaction would be followed by the formation of silicate ion, ($2 \text{OH}^- + \text{SiH}_4 + \text{H}_2\text{O} = 4 \text{H}_2 + \text{SiO}_3^{2-}$) which is thermodynamically stable throughout the potential range. The unusual - but entirely reasonable - feature of the proposed reaction is that the reduction of Si to SiH_4 promotes the formation of SiO_3^{2-} . The diffusion of SiH_4 or SiO_3^{2-} from the electrode may then be responsible for the observed enhancement of the rate by stirring. At sufficiently high potentials Tafel behavior is observed with $i_0 = 10^{-7} \text{ A/cm}^2$ and $b = 180 \text{ mV}^*$.

NiSi in both acid and alkaline solutions exhibit none of the peculiarities associated with elemental silicon. The polarization is characteristic of the h. e. r. The Tafel parameters in acid are $b = 113 \text{ mV}$ and $i_0 = 4 \times 10^{-6} \text{ A/cm}^2$, which are similar to those on nickel itself. The data at pH 10.8 exhibit hysteresis, with the overpotential in the direction of decreasing current exceeding that in the reverse direction. The exchange current is $\sim 10^{-5} \text{ A/cm}^2$, i. e., about the same as on Ni, but the Tafel slope is $\sim 160 \text{ mV}$.

*Further evidence for the proposed scheme is the well-known corrosion of Si in alkaline solution. According to the present data the hydrogen overpotential on Si in alkaline solutions is such that corrosion currents exceeding 10^{-4} A/cm^2 could not be supported by the h. e. r. It appears, therefore, that the cathodic component of the normal corrosion reaction may be the reduction of Si to SiH_4 .

NiAs and As

In acid solutions NiAs exhibits Tafel behavior in the range 2×10^{-5} - 2×10^{-3} A/cm² with $b = 56$ mV, and $i_o = 5 \times 10^{-8}$ A/cm². The polarization curve thus crosses that of Ni (Fig. 3).

The high resistivity of elemental arsenic prohibits the direct measurement of hydrogen overpotential on the arsenic electrode. An estimate of the Tafel parameters for the h. e. r. on arsenic was obtained by the following procedure: 10^{-3} M/l As₂O₃ was added to a solution with a nickel electrode biased at -300 mV. The current diminished slowly to a steady-state value of 3×10^{-6} A/cm². Polarization measurements then revealed Tafel behavior in the range 10^{-6} to 3×10^{-5} A/cm² with $b = 120$ mV and $i_o = 10^{-8}$ A/cm², the results being unaffected by stirring. Between 2×10^{-4} and 2×10^{-3} A/cm² (galvanostatic measurements were specially employed) the potential became independent of current. However, the polarization curve in this current range exhibits an extraordinary dependence on stirring, viz., the overpotential increases with stirring. As the current is increased beyond 10^{-2} A/cm², the curves approach that of Ni, regardless of stirring.

We offer the following interpretation of these results. As₂O₃ is unstable with respect to As at all negative potentials: $\text{As}_2\text{O}_3 (\text{aq}) + 6 \text{H}^+ + 6 \text{e} = 2\text{As} + 3 \text{H}_2\text{O}$; $E_o = +0.247 \text{ V}$ ⁽¹⁶⁾. We assume accordingly that As is deposited upon the nickel surface, but that the reaction stops at monolayer coverage, because of a high overpotential for reduction of As₂O₃ on As. The residual current is then due to the h. e. r. on a chemisorbed arsenic monolayer. It is also possible that the steady-state current is due to the h. e. r. on a small residue of bare nickel, although this seems improbable. As the potential is increased, the reduction of As to AsH₃ becomes thermodynamically feasible, $(\text{As} + 3 \text{H}^+ + 3 \text{e} = \text{AsH}_3; E_o = 0.60 \text{ V})$ ⁽¹⁶⁾. The formation of AsH₃ would compete with the h. e. r. exposing bare Ni. The C.D. would then increase toward the value characteristic of the h. e. r. on Ni. Counteracting this effect will be the diffusion of fresh AsO₃ to the surface and the restoration of the As film. Stirring will assist diffusion and will thus oppose the tendency to increased h. e. r. currents. At sufficiently high C.D.'s, the formation of AsH₃ becomes more rapid than the diffusion rate so that the surface will remain effectively free of As,

regardless of stirring. The polarization curve will then approach that of the h. e. r. on pure nickel. Our suggestion that the deposition of As is limited to a monolayer is based on the observation that prolonged electrolysis at -300 mV does not affect the results.

In alkaline solutions NiAs exhibits some hysteresis, but generally obeys the Tafel relation with $b = 155$ mV and $i_0 = 7 \times 10^{-7}$ A/cm². In contrast to the results in acid solution, addition of 10^{-3} M/1 As₂O₃ has no effect on the h. e. r. on nickel electrodes.

NiSb and Sb

In acid solutions NiSb exhibits a Tafel behavior with $b = 108$ mV and $i_0 = 2 \times 10^{-8}$ A/cm² over the C. D. range 5×10^{-5} to 10^{-2} A/cm². (Fig. 4). At lower currents, the overpotential is less than that extrapolated from the Tafel line and is time dependent. In the case of Sb there is evidence for Tafel behavior only at currents exceeding 10^{-3} A/cm² (with $b \sim 180$ mV and $i_0 = 2 \times 10^{-6}$ A/cm²). At lower currents, there is a sharp drop to lower overpotentials; the currents in this region ($|E| < 0.4$ V) are steady and still substantial, thus ruling out cathodic depolarization by the reduction of traces of oxygen or by the reduction of a residual surface oxide. This general effect is even more pronounced in alkaline solution. Here the break occurs at a higher overpotential ($|E| \sim 0.5$ V) and the approach to a steady-state current is very slow. Since the antimony oxides are all unstable at negative potentials⁽¹⁶⁾, the results, which are similar to those observed by others⁽¹⁷⁾, are explicable only in terms of hydride formation. However, the reported potentials for the formation of SbH₃ are too negative so that a lower hydride, e. g., Sb₂H₄, may be involved.

Tafel behavior with values of $b \sim 250$ mV are observed in alkaline solution for both NiSb and Sb. NiSb also shows an apparent depolarization at $|E| < 150$ mV, i. e., cathodic currents are observed at potentials positive to the reversible hydrogen electrode.

NiS and Ni/H₂S

The results for these systems are given in Fig. 5. NiS in acid solution follows the Tafel relationship between 3×10^{-5} and 10^{-2} A/cm², with

$b = 62$ mV and $i_0 = 7 \times 10^{-8}$. The polarization curve thus crosses that of Ni. The odor of H_2S was detected in the effluent gas stream during these runs. The addition of 10^{-3} M/l Na_2S to the solution had no effect on the polarization curve.

The addition of 10^{-3} M/l Na_2S to an acid solution has a strong and reproducible tendency to shift the polarization characteristics of a nickel electrode towards that of NiS.

In alkaline solution the behavior of NiS closely resembles that of Ni. The addition of Na_2S to alkaline solution has no apparent effect on Ni.

NiTe₂ and Te

Experiments were limited to acid solutions, and are summarized in Fig. 6. The results for Te, which are highly reproducible, show the same apparent depolarization as observed for Sb. Similar results have been observed by Awad⁽¹⁸⁾ who tried to explain them by postulating the formation of an intermediate hydride, H_2Te_2 .

NiTe₂ shows some evidence of a break in the Tafel curve at the same potential where Te exhibits its transition. The Tafel parameters for Te are $b \sim 48$ mV, and $i_0 \sim 10^{-11}$ A/cm², while those for NiTe₂ are $b \sim 55$ mV, and $i_0 \sim 10^{-8}$ A/cm². The uncertainty in the value of i_0 for NiTe₂ is considerable, however, and its polarization curve can be virtually superposed on that of Te by a shift in the abscissa.

IV. DISCUSSION

Under the present experimental conditions, the cathodic reaction on nickel electrodes is confined to the hydrogen evolution reaction. In all other cases, excepting silicon, the h. e. r. is also dominant over extended potential regions, giving rise to Tafel behavior, i. e., $\eta = -b \log i/i_0$ where η is the overpotential relative to the reversible hydrogen electrode, b is the Tafel slope, and i_0 is the exchange current. The values of these parameters, and their range of applicability, are summarized in Table I.

The cathodic polarization curves on each of the elements, except nickel, exhibit features which suggest side reactions such as hydride formation or oxide reduction. In the case of Sb, these features are partially

reflected in the behavior of NiSb. However, NiAs, NiTe₂, and NiSi do not show significant side effects, illustrating that the surface chemical reactions of As, Te, and Si atoms are basically conditioned by their particular crystal environment. Since the kinetics of h. e. r. on the compounds differ from those on Ni itself, it is unlikely that the absence of side reactions on a nickel compound can be attributed simply to chemical depletion of the companion element in the surface region. We shall not dwell on the side reactions, however, but shall limit our discussion to a resolution of the atomic and crystal contributions to the h. e. r.

Atomic Approach

In the simplest atomic approximation it is assumed that each of the surface atoms reacts independently. The overall reaction rate at a specified potential would then be given by a linear combination of the contributions of the component atoms. These contributions may be estimated from the behavior of the elemental electrodes, proper account being made of the relative surface concentrations on the elements and the compound.

In the cases of NiAs, NiTe₂, and NiSi in acid solution, there are potential regions where the C. D. 's on the compounds are greater than on either of the component elements. This immediately rules out the simple atomic description since the surface concentration of either component, regardless of crystallographic orientation, does not exceed that of its elemental form. The electrodes have interesting qualitative features, however. The general shape of the Tafel line on NiTe₂ resembles that of Te, while a similar correspondence exists for NiSi and Ni. This implies that the mechanism for these systems is determined by only one of the components, suggesting in turn that the surface consists predominantly of this component. The effect may originate from anisotropic corrosion leading to the exposure of a stable crystallographic plane in which only one component is present. This phenomenon is now well documented for III-V intermetallic compounds such as InSb and GaAs, and leads to striking differences of chemical reactivity on opposite (111) crystallographic surfaces⁽²⁾. However, both the stability of the Si-O bond and the hydride formation indicated for elemental tellurium would argue against the requisite configurations on NiSi and NiTe₂. In any

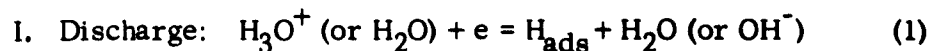
event, it would still be necessary that the rate of the h. e. r. on Ni atoms in NiSi, and Te atoms in NiTe₂, be faster than on the corresponding elemental crystals. In these cases, then, atomic properties may govern the mechanism of the reaction, but crystal properties apparently govern the magnitude of the reaction rate.

Similar considerations may also apply to NiS. However, the experimental results for the h. e. r. on "sulphur" were obtained by exposing a nickel electrode to H₂S. Since H₂S was also detected in the gas stream coming from the cell in which NiS was under study, it is not improbable that the latter may in fact be equivalent to the "Ni + H₂S" electrode. In alkaline solution, however, H₂S has no effect on the polarization behavior of Ni which indicates that H₂S is not adsorbed on the electrode. The NiS electrode behaves similarly to nickel, although the h. e. r. proceeds at a smaller rate; it is plausible that sulphur in the surface region of NiS is removed by electrochemical discharge of H₂S (NiS + 2H₂O = H₂S + 2OH⁻ + Ni; E₀ = - 0.77 V).

For the remaining cases under study, it is evident that the overall rate of the h. e. r. is not a specific atomic property, and that interactions between the surface atoms or between adsorbed hydrogen atoms at neighboring sites on the crystal surface play a prominent role. It is possible, however, that the atomic approach may still be valid for one or more of the reaction steps in the overall mechanism. In order to elucidate this possibility we shall briefly discuss the generally acknowledged mechanism of the h. e. r.

Mechanism of the Hydrogen Evolution Reaction ⁽¹⁹⁾

It is self-evident from its stoichiometry and its heterogeneous character that the hydrogen evolution reaction involves one or more reaction intermediates which are adsorbed at the electrode surface. By analogy to gas-phase dissociative chemisorption of hydrogen it has long been supposed that the predominant intermediate is an adsorbed hydrogen atom which is produced by the reduction of an adsorbed hydronium ion or water molecule, i. e. ,

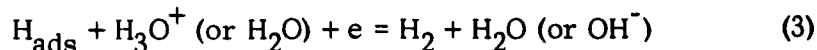


The discharge step may be followed by a bimolecular combination of H_{ads}, i. e. ,



or an electrochemical desorption step,

III. Electrochemical desorption:



Other intermediates have been proposed. In particular, Horiuti has theorized that the adsorbed hydrogen-molecule ion, H_2^+ , may play an important role for many electrodes⁽²⁰⁾. This species may be regarded formally as a stable intermediate in III.

The reaction kinetics involve the quantity θ , which is the fractional coverage of the available surface by hydrogen atoms. The cathodic current is given by:

$$V_{\text{I}} = k_{\text{I}}^{\circ} (1 - \theta) e^{-\alpha\eta\bar{f}/RT} \quad (4)$$

$$V_{\text{II}} = k_{\text{II}}^{\circ} \theta^2 \quad (5)$$

$$V_{\text{III}} = k_{\text{III}}^{\circ} \theta e^{-\alpha\eta\bar{f}/RT} \quad (6)$$

where the k 's are specific rate constants, and α is a transfer coefficient.

At equilibrium, i. e., $\eta = 0$, the rates of I, II, and III are given by:

$$i_{\text{O}}^{\text{I}} = k_{\text{I}}^{\circ} (1 - \theta_{\text{O}}) \quad (7)$$

$$i_{\text{O}}^{\text{II}} = k_{\text{II}}^{\circ} \theta_{\text{O}}^2 \quad (8)$$

$$i_{\text{O}}^{\text{III}} = k_{\text{III}}^{\circ} \theta_{\text{O}} \quad (9)$$

where θ_{O} , the equilibrium coverage, is determined by the free energy of adsorption of H_2 on the particular electrode in the particular solution. When i_{O}^{I} is much smaller than either i_{O}^{II} or $i_{\text{O}}^{\text{III}}$, the reaction kinetics are controlled by slow discharge and do not depend upon the mechanism of desorption. Adsorbed hydrogen comes to equilibrium with the ambient gas by Step II, and θ remains independent of η . Eq. (4) or (6) reduces to the Tafel equation with $b = 2.3 RT/\alpha\bar{f} = (59/\alpha)\text{mV}$ at 25°C . There is strong empirical evidence that α generally approximates $1/2$ ⁽¹⁹⁾ so that $b \approx 120 \text{ mV}$.

When II is rate-controlling, the rate is given by Eq. (5). With increasing overpotential θ increases as

$$\theta \simeq \theta_0 e^{-\eta F/RT} \quad (10)$$

This result may be substituted in Eq. (5) and leads to a Tafel equation with $b = 2.303 RT/2F = 29 \text{ mV}$ at 25°C . Finally, when III is rate-limiting, substitution of Eq. (10) into Eq. (6) leads to a Tafel equation with $b = 2.3 RT/\gamma$ where γ is believed to change from $3/2$ ($b \sim 40 \text{ mV}$) at low θ to $1/2$ ($b \sim 120 \text{ mV}$) at high θ ⁽¹⁹⁾.

An explicit test of the various mechanisms requires an experimental determination of θ vs. η . This has been carried out by Devanathan and Selvaratnam⁽²¹⁾ for Ni in 2N NaOH and Makrides⁽²²⁾ has shown that the data, which exhibit a change in θ from 0.04 to 0.4 as η is increased from 40 to 200 mV, can be explained on the assumption $i_0^I \sim i_0^{II} \gg i_0^{III}$. Because of the relative values of b , the discharge step plays the prime role in molding the kinetics. The case of Ni in acid solution has not been clarified, but it is generally believed that slow discharge controls the kinetics⁽¹³⁾.

It is apparent from the foregoing that the association of two different atoms in an intermetallic compound could lead to a basic modification in the kinetics of a surface reaction, even though the reactivity is inherently an atomic property. Thus, it is conceivable that discharge could be faster on atoms of one element, say A, while electrochemical desorption may be faster on the second element, B. In this case, if discharge on A were followed by transfer to a neighboring B atom, the overall rate of the h. e. r. on the compound AB would be faster than on either element by itself. In the event that desorption proceeds through II, the effect could be even more pronounced since combination desorption requires the juxtaposition of two adsorbed hydrogen atoms, a process which will be strongly conditioned by the atomic configuration of the surface. In this way specific atomic properties may still underlie the kinetics, although the rates on the compound and on its elemental constituents may differ significantly. A clear distinction can still be made between the case of a compound and of a physical admixture of two elemental phases where in the absence of significant grain boundary effects, the rate must be given by a linear combination of the rates on the elements.

For example, Ni chemisorbs H_2 dissociatively at room temperature while As does not react measurably under the same conditions⁽²⁴⁾. Since the bond energies of Ni-H and As-H are similar, the difference must be in the activation energy for dissociative chemisorption. This difference should apply as well to the activation energy for the reverse reaction which is identical to II. It is thus reasonable that II would be strongly inhibited by the presence of As, and that the desorptive mechanism might shift from II to III. This would apply whether the arsenic were present as chemisorbed atoms or as a fundamental crystal constituent, as in NiAs.

The case of NiAs is particularly interesting since it exhibits Class A behavior, although the individual elements show Class B behavior. While the h. e. r. on Ni is presumed to be limited by the discharge rate, the rate-limiting step on As is open to conjecture. According to the foregoing reasoning, III will likely control the rate. Supporting this contention is the fact that, if discharge were rate-limiting, $i_O^I(As)/i_O^I(Ni) \sim 10^{-3}$; this ratio is exceptionally small in view of the fact that the energies of adsorption and the work functions⁽²⁵⁾, both of which should affect i_O^I , are apparently similar for Ni and As. Assuming rate-control by III, the As film must be nearly saturated with hydrogen atoms, i. e., $\theta \rightarrow 1$, to account for a Tafel slope of 120 mV.

We suggest, therefore, that the h. e. r. on As proceeds by I + III. The same factors which underlie this, namely localized adsorption, should persist in NiAs, particularly since the As-As distance on an arsenic monolayer on Ni and the Ni-As distance in NiAs are similar⁽⁹⁾. One would expect then that the h. e. r. reaction on As atoms in NiAs proceeds independently of the reaction on nickel. The association of Ni and As has two important effects, however. First, it inhibits II on the Ni atoms by sharply reducing the number of near Ni-Ni neighbors, and shifts the desorption mechanism to III. Secondly, it increases the discharge rate on nickel itself by about an order of magnitude as shown by the experimental results.

While the decrease in the rate of an elementary electrochemical step such as I or III might be discussed as an artifact of adventitious inhibition, an enhancement of the rate obviously requires a change in the basic properties of the surface. This effect, which is common to many of the

present results, may, in the simplest instance, be related to the work function ϕ_m of the electrode. Thus, the energy state of a hydrogen ion in solution relative to a reference phase of H_2 gas, varies with ϕ_m^* . This affects the exchange current, and should lead in zeroth approximation to the relation:

$$-\log i_0^I = \text{const.} + C \phi_m$$

where $C \sim RT/2.3 \sim 9(\text{ev})^{-1}$. The experimental results for the h. e. r. on a series of transition metals shows⁽¹⁹⁾ that $C \sim 2.5 (\text{ev})^{-1}$, which means that other significant changes accompany the variation of ϕ . In any event, an increase of 0.5 ev in the electrode work function would be expected on empirical grounds alone to bring about an order of magnitude increase in i_0^I . This is not an implausible consequence of the chemical liaison between Ni and As, both of which individually show $\phi_m \sim 5.0$ ev.

Despite the similar crystal structure of NiAs and NiSb, the latter exhibits Class B behavior in acid solutions. A self-consistent explanation would be that slow discharge on the Ni atoms is rate-controlling on NiAs, but with an exchange current which is 10-fold smaller than on elemental nickel. This result may also stem from a decrease in ϕ_m . It also seems likely that slow discharge controls the rate on NiSi in acid solution, requiring that $\phi_{\text{NiSi}} > \phi_{\text{Ni}}$.

In the case of NiTe_2 and NiSi in acid solution, the h. e. r. appears to be dominated by electrochemical desorption on the Group VI atoms. Assuming that the rate of I on these materials is inherently faster, one would deduce that i_0^I increases in the order: NiSb, Ni, NiS \sim NiTe_2 , NiSi, NiAs. There is, however, no simple correlation with chemical factors, such as electronegativity difference, or the energy of compound formation⁽²⁷⁾ which might be expected to influence ϕ_m .

The situation in alkaline solutions is even more complex. For all compounds, the Tafel slope is higher than in acid solutions, which may indicate a shift in mechanism. Alternatively, the magnitude of b may be taken to signal a change in the structure of the electrolytic double layer, for

*This arises since equilibrium for the reaction $1/2 H_2(g) = H^+(aq) + e(\text{metal})$ requires that $1/2 \mu_{H_2} - \mu_{H^+} = \mu_e$, and μ_e is a direct measure of ϕ_m in metals⁽²⁵⁾.

example, of specific adsorption of hydroxyl ions. In the case of NiAs, where the exchange current is smaller by two orders of magnitude than on nickel, the changes in work function and interatomic distances discussed above imply that the polarization curve in alkaline solution is determined by electrochemical desorption at high θ . This conjecture may be viewed in light of the fact that Ni itself shows high θ in the potential range in question⁽²¹⁾ despite the inherently less favorable condition (for achieving high θ) that desorption on Ni is by reaction II rather than by reaction III.

In conclusion, the electrocatalysis of the h. e. r. on nickel compounds cannot be explained in terms of the intrinsic chemical properties of the surface atoms. The most pointed demonstration is that the overall rate of reaction at a given potential is frequently greater than on either of the individual elements. Nevertheless, the atomic approach is a useful point of departure for interpreting the effects of composition and crystal structure upon electrocatalytic activity. The use of this approach was illustrated for NiAs, NiTe₂, and NiSi. Further work along these lines, together with complementary studies of the electronic properties and gas phase chemisorption characteristics, promises to be useful from both a scientific and a technical standpoint.

Acknowledgments

The authors wish to acknowledge the expert technical assistance of Miss Mary Loud and Miss MaryJane MacLaren and the valuable technical comments of Dr. A. C. Makrides.

REFERENCES

- 1 Rosenberg, A. J., J. Phys.Chem.Solids, 14, 175 (1960)
- 2 Gatos, H. C., Science, 137, 311 (1962)
- 3 Gatos, H. C., and Lavine, M. C., J. Electrochem. Soc., 107, 427 (1960)
- 4 Dowden, D. A., J. Chem. Soc., 242 (1950)
- 5 Hauffe, K., ""Advances in Catalysis", Vol.7, 1955, p.213
- 6 Randles, J. E. B., and Somerton, K. W., Trans. Faraday Soc., 48, 937, 951 (1952)
- 7 Stern, M., and Wissenberg, H., J. Electrochem.Soc., 106, 759 (1959)
- 8 Brattain, W. H., and Garrett, G. G. B., Bell System Tech. J., 34, 129 (1955)
- 9 Pearson, W. B., "Handbook of Lattice Spacing and Structures of Metals and Alloys", Pergamon Press, 1958
- 10 Cornish, A. J., Acta Metallurgica, 6, 371 (1958)
- 11 Hansen, M., "Constitution of Binary Alloys", 2nd Ed., McGraw-Hill, 1958
- 12 "KEL-F Brand Polymer Wax, Grade KF 200" obtained from Chemical Div., Minnesota Mining & Manufacturing Co., St. Paul, Minn.
- 13 Bockris, J. O'M., and Potter, E. C., J. Chem. Phys., 20, 614 (1952)
- 14 Latimer, W. M., "Oxidation Potentials", 2nd Ed., Prentice Hall, Inc., 1959
- 15 Turner, D. R., "Electrochemistry of Semiconductors", Ed. J. P. Holmes, Academic Press, 1961
- 16 Ref. 14
- 17 Piontelli, R., et al. "Research on Hydrogen Overvoltage on Metallic Single Crystal", Tech. Documentary Report No. ASD TN 61-158, March 1962, Contract No. AF 61 (052)-144
- 18 Awad, S. A., J. Phys. Chem., 66, 890 (1962)
- 19 Bockris, J. O'M., "Modern Aspects of Electrochemistry", Vol. 1, Butterworth, London, 1954
- 20 Horiuti, J., "Trans. Symposium on Electrode Processes", Ed. E. Yeager, John Wiley & Sons, Inc., New York, 1961, p.17
- 21 Devanathan, M. A. V., and Selvaratnam, M., Trans. Faraday Soc., 56, 1820 (1960)
- 22 Makrides, A. C., J. Electrochem. Soc., 109, 977 (1962)
- 23 Pauling, L., "The Nature of Chemical Bonds", Cornell Univ. Press, New York, 3rd Ed., 1960

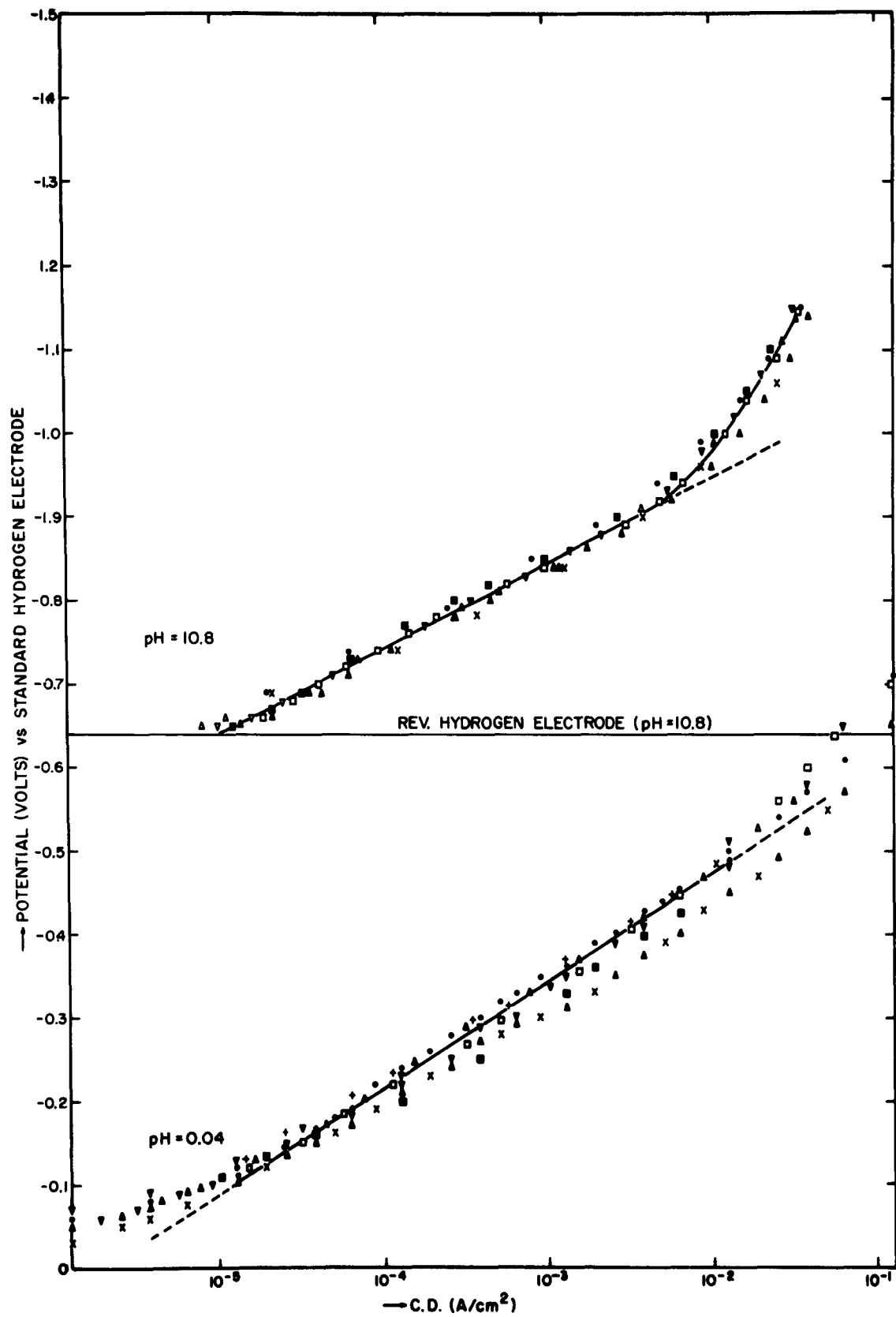
- 24 Trapnell, B.M.W. , "Chemisorption", Butterworths, London, 1955
- 25 "Handbook of Chemistry and Physics", 41st Ed. , Chemical Rubber Publishing Co. , 1960, p. 2557
- 26 Bockris, J.O'M. , and R. Parsons, Trans. Faraday Soc. , 47, 914 (1951)
- 27 Raynor, G.F. , "The Physical Chemistry of Metallic Solutions and Intermetallic Compounds", Vol. 1, p. 312, Chemical Publishing Co., New York, 1960

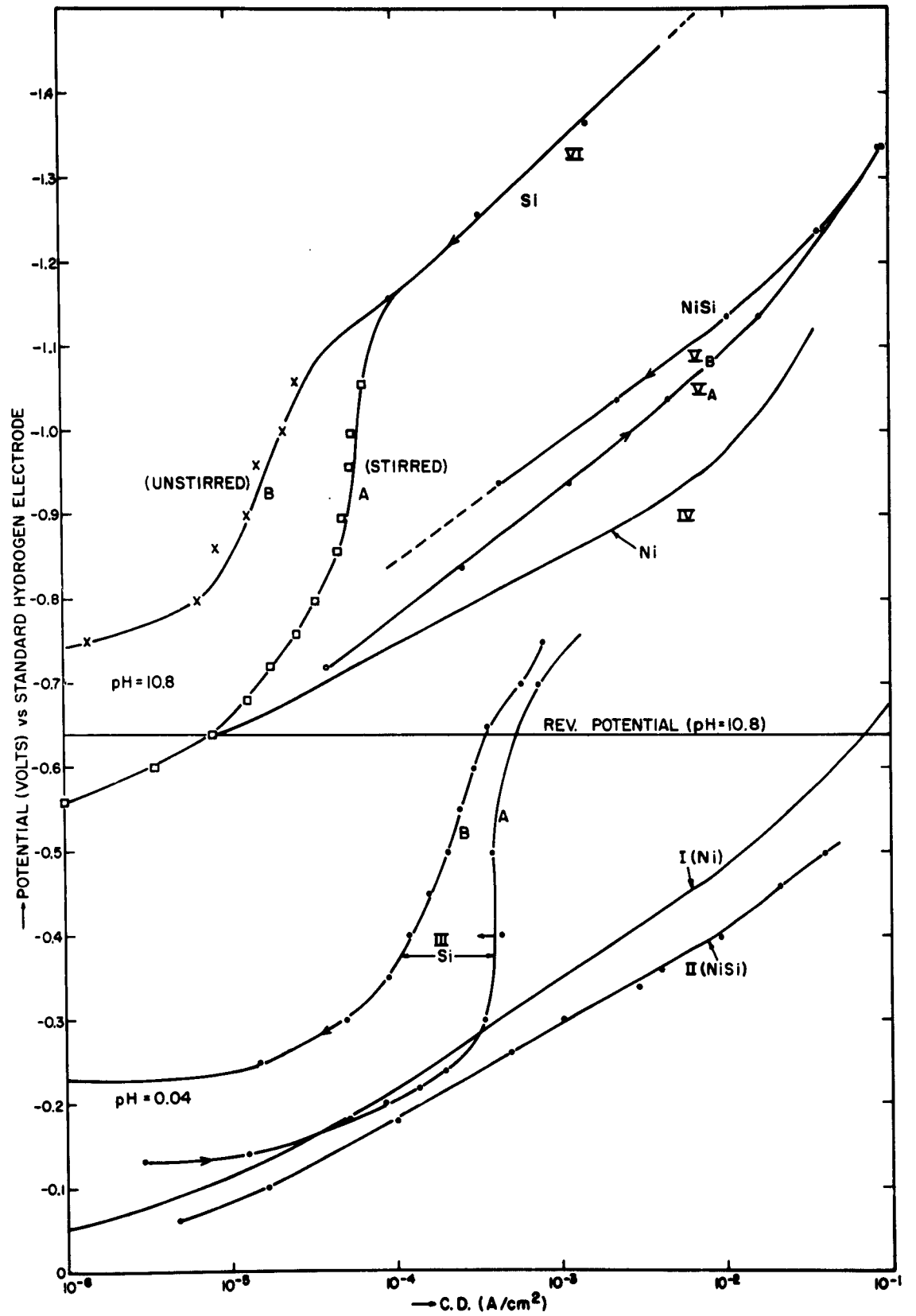
FIGURE CAPTIONS

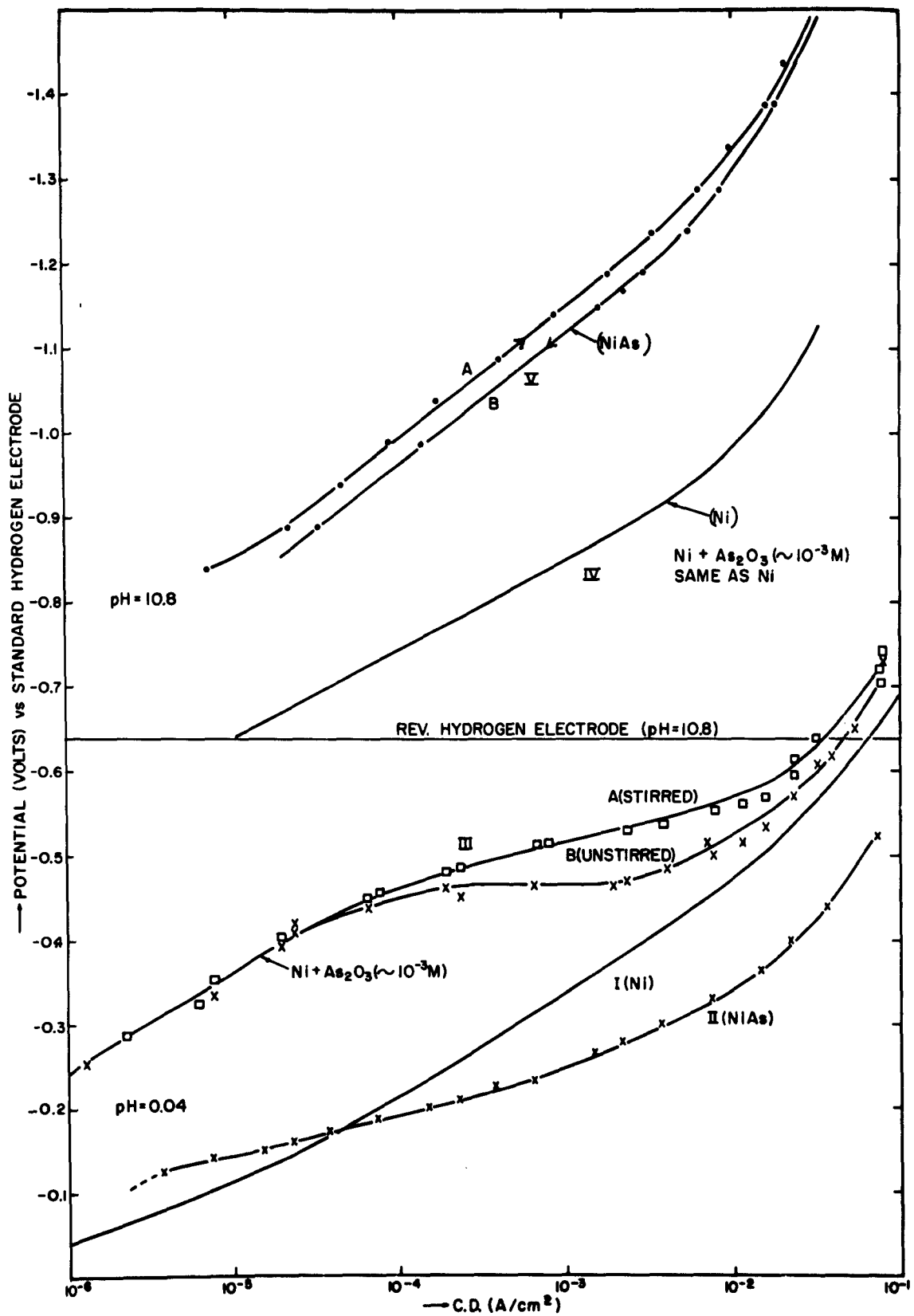
- Fig. 1 H. e. r. on nickel in 1 M HClO_4 , pH = 0.04 and in 1 M $\text{NaClO}_4 + 10^{-2}$ M NaOH, pH = 10.8 at 25°C. Solution preelectrolyzed at 30 ma for 16 hours. Results of ten runs at pH = 0.04 with mean $b = 0.125$ V, $i_0 = 2 \times 10^{-6}$ A/cm² and of six runs at pH = 10.8 with $b = 0.105$ V, $i_0 = 1 \times 10^{-5}$ A/cm²
- Fig. 2 Cathodic polarization curves (log C. D. vs. potentials) for NiSi and Si in 1 M HClO_4 , pH = 0.04, and in 1 M $\text{NaClO}_4 + 10^{-2}$ M NaOH, pH = 10.8 at 25°C. At pH = 0.04, I - Ni (for comparison), II - NiSi, III_A - Si towards higher cathodic potentials (up), III_B - Si, towards lower cathodic potentials (down). At pH = 10.8, IV - Ni (for comparison), V_A - NiSi (up), V_B - NiSi (down), VI - Si (A-stirred, B-unstirred)
- Fig. 3 Cathodic polarization curves (log C. D. vs. potentials) for NiAs and Ni + 10^{-3} M As_2O_3 in 1 M HClO_4 , pH = 0.04, and in 1 M $\text{NaClO}_4 + 10^{-2}$ M NaOH, pH = 10.8 at 25°C. At pH = 0.04, I - Ni, II - NiAs, mean of 5 runs, III - Ni with addition of $\sim 10^{-3}$ M As_2O_3 in solution; (A-stirred, B-unstirred). At pH = 10.8, IV - Ni, no effect of $\sim 10^{-3}$ M As_2O_3 added to solution. V - NiAs (A-"up", B-"down")
- Fig. 4 Cathodic polarization curves (log C. D. vs. potentials) for NiSb and Sb in 1 M HClO_4 , pH = 0.04, and in 1 M $\text{NaClO}_4 + 10^{-2}$ M NaOH, pH = 10.8 at 25°C. At pH = 0.04, I - Ni, II - NiSb, III - Sb. At pH = 10.8, IV - Ni, V - NiSb, VI - Sb. (A - "up", and B- "down")
- Fig. 5 Cathodic polarization curves (log C. D. vs. potentials) in 1 M HClO_4 , pH = 0.04 and in 1 M $\text{NaClO}_4 + 10^{-2}$ M NaOH, pH = 10.8 at 25°C. At pH = 0.04, I - Ni, II - NiS (odor of H_2S in the effluent gas), III - Ni in presence of H_2S , added as Na_2S . At pH = 10.8, IV - Ni, V - NiS, no effect of addition of $\sim 10^{-3}$ M Na_2S

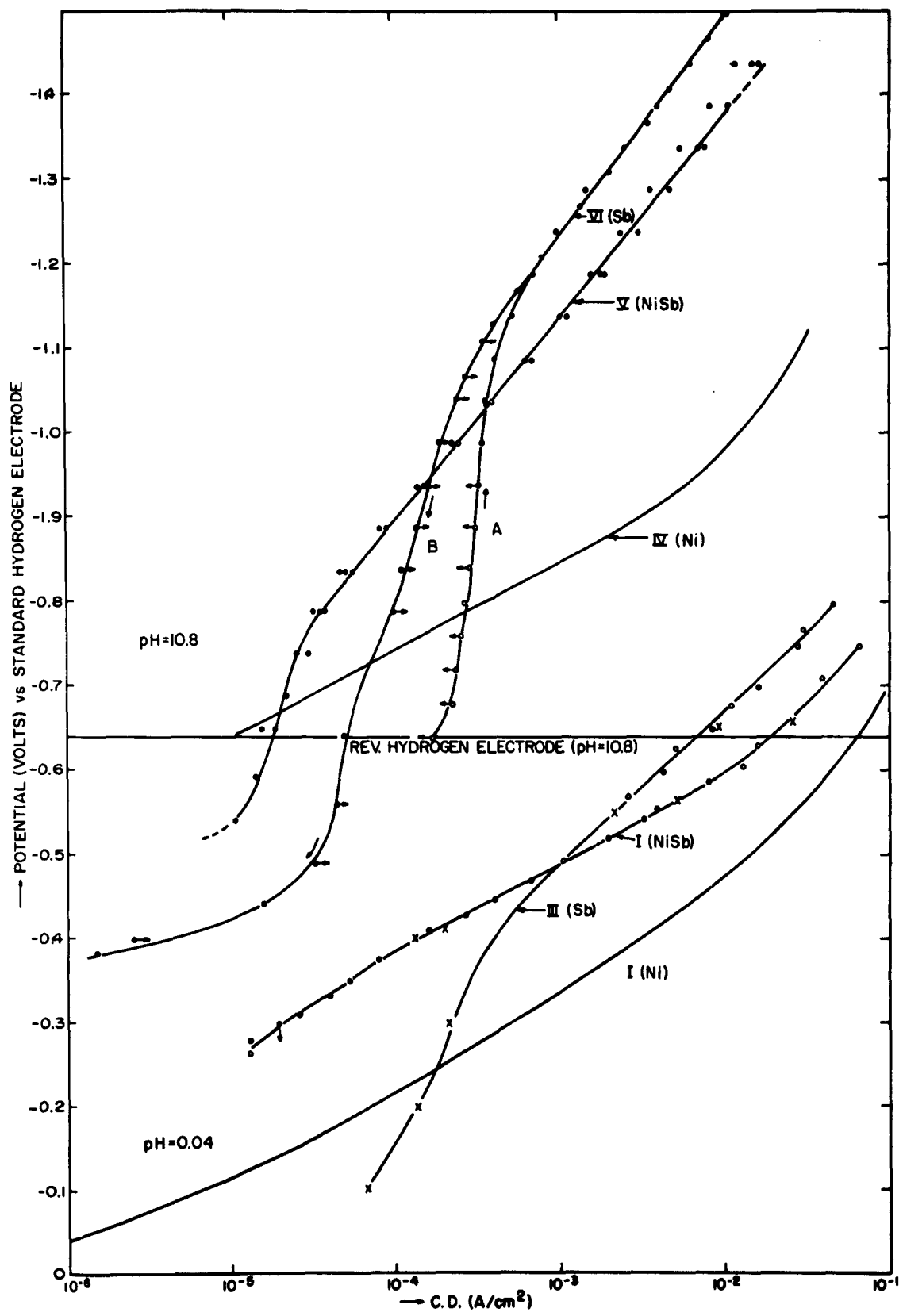
FIGURE CAPTIONS - continued

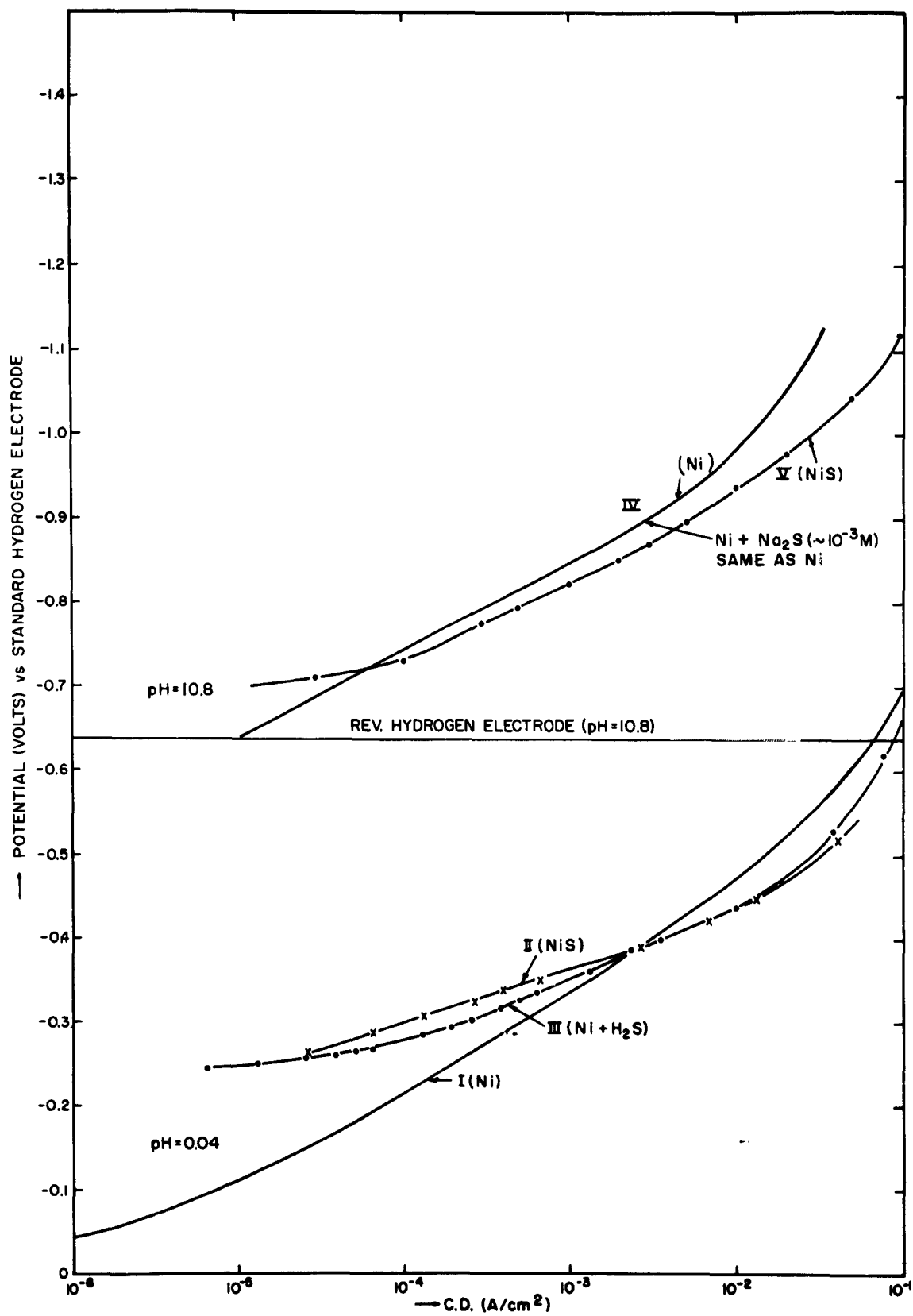
Fig. 6 Cathodic polarization curves (log C. D. vs. potentials) in
1 M HClO_4 , pH = 0.04, at 25°C. I - Ni, II - NiTe_2 ,
III - Te.











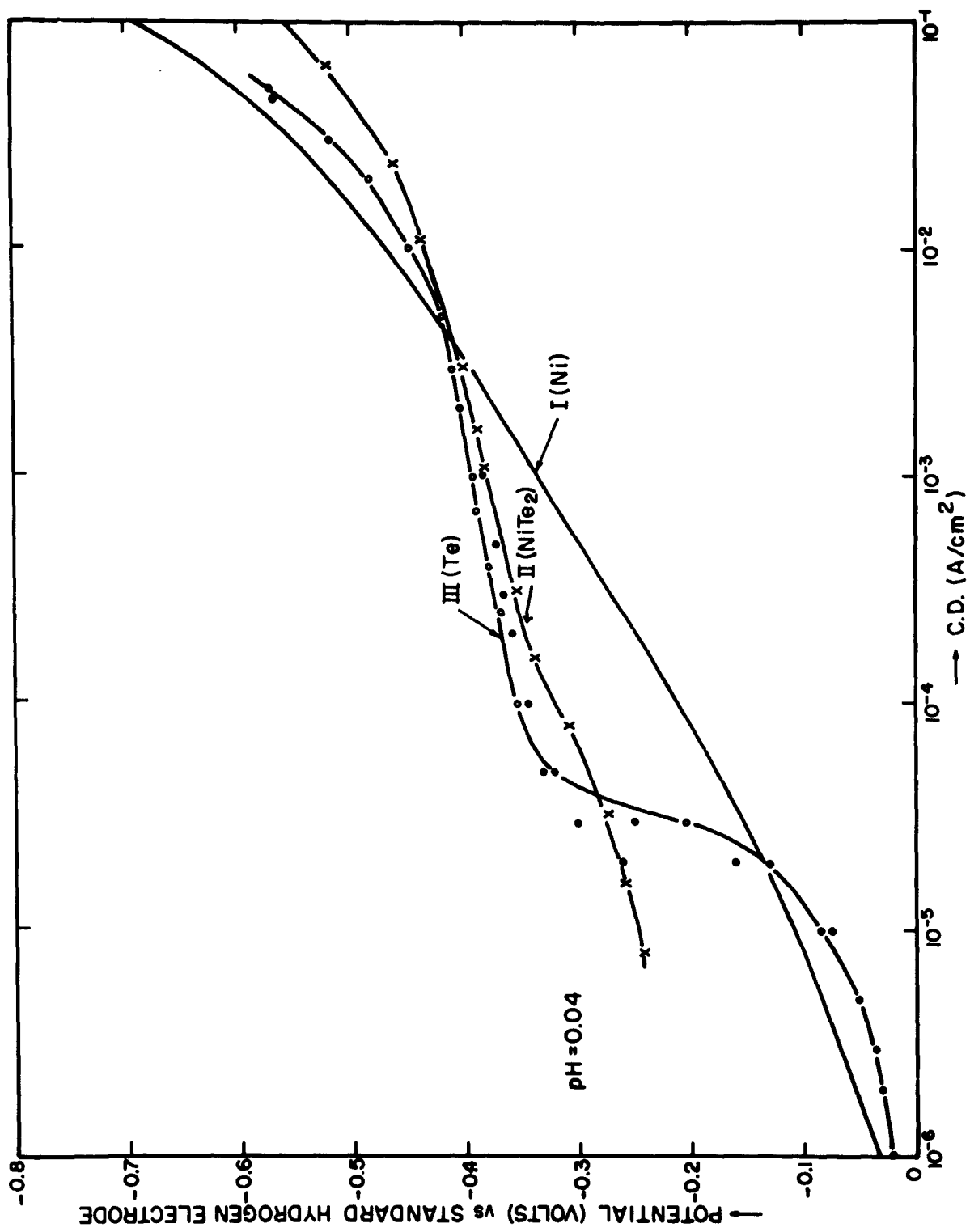


TABLE I
Tafel Parameters for the Hydrogen Evolution Reaction

		<u>b(mv)</u>	<u>i_0 (A/cm²)</u>	<u>range of i (A/cm²) for b</u>
Ni	Acid	125	2×10^{-6}	$4 \times 10^{-5} - 3 \times 10^{-3}$
	Alkaline	105	1×10^{-5}	$1.5 \times 10^{-5} - 5 \times 10^{-3}$
NiSi	Acid	113	4×10^{-6}	$5 \times 10^{-5} - 10^{-1}$
	Alkaline	145	3.5×10^{-6}	$5 \times 10^{-4} - 10^{-2}$
Si	Acid	-	-	-
	Alkaline	168	3×10^{-8}	$10^{-4} - 5 \times 10^{-3}$
NiSb	Acid	108	2.5×10^{-8}	$5 \times 10^{-5} - 10^{-2}$
	Alkaline	245	$\sim 10^{-5}$	$3 \times 10^{-5} - 2 \times 10^{-2}$
Sb	Acid	170	2×10^{-6}	$7 \times 10^{-4} - 2 \times 10^{-2}$
	Alkaline	260	5×10^{-6}	$3 \times 10^{-4} - 10^{-2}$
NiAs	Acid	56	5×10^{-8}	$2.5 \times 10^{-6} - 2.5 \times 10^{-3}$
	Alkaline	155	7×10^{-7}	$10^{-5} - 5 \times 10^{-3}$
Ni	Acid + As ₂ O ₃	120	10^{-8}	$10^{-6} - 2 \times 10^{-5}$
	Alk. + As ₂ O ₃	105	1×10^{-5}	$1.5 \times 10^{-5} - 5 \times 10^{-3}$
NiS	Acid	62	7×10^{-8}	$3 \times 10^{-5} - 10^{-2}$
	Alkaline	100	1.3×10^{-5}	$10^{-4} - 5 \times 10^{-3}$
Ni	Acid + H ₂ S	80	4×10^{-8}	$2 \times 10^{-4} - 5 \times 10^{-3}$
	Alk. + Na ₂ S	105	1×10^{-5}	$1.5 \times 10^{-5} - 5 \times 10^{-3}$
NiTe ₂	Acid	55	10^{-8}	$10^{-4} - 10^{-2}$
Te	Acid	48	10^{-11}	$10^{-4} - 10^{-2}$

TECHNICAL REPORT DISTRIBUTION LIST

Contract No. Nonr 3765(00)

Commanding Officer Office of Naval Research Branch Office The John Crerar Library Building 86 East Randolph Street Chicago 1, Illinois (1)	Air Force Office of Scientific Research (SRC-E) Washington 25, D. C. (1)
Commanding Officer Office of Naval Research Branch Office 346 Broadway New York 13, New York (1)	Commanding Officer Diamond Ordnance Fuze Labs. Washington 25, D. C. Attn: Technical Information Office Branch 012 (1)
Commanding Officer Office of Naval Research Branch Office 1030 East Green Street Pasadena 1, California (1)	Office, Chief of Research & Development, Dept. of the Army Washington 25, D. C. Attn: Physical Sciences Div. (1)
Commanding Officer Office of Naval Research Branch Office Box 39 Navy #100 Fleet Post Office New York, New York (7)	Chief, Bureau of Ships Department of the Navy Washington 25, D. C. Attn: Code 342C (2)
Director, Naval Research Laboratory Washington 25, D. C. Attn: Technical Information Officer (6) Chemistry Division (2)	Chief, Bureau of Naval Weapons Department of the Navy Washington 25, D. C. Attn: Technical Library (4)
Chief of Naval Research Department of the Navy Washington 25, D. C. Attn. Code 425 (2)	ASTIA Document Service Center Arlington Hall Station Arlington 12, Virginia (10)
DDR&E Technical Library Room 3C-128, The Pentagon Washington 25, D. C. (1)	Director of Research U. S. Army Signal Research & Development Laboratory Fort Monmouth, New Jersey (1)
Technical Director Research & Engineering Division Office of the Quartermaster General Department of the Army Washington 25, D. C. (1)	Naval Radiological Defense Laboratory San Francisco 24, California Attn: Technical Library (1)
Research Director Clothing & Organic Materials Division Quartermaster Research & Engineering Command, U. S. Army Natick, Massachusetts (1)	Naval Ordnance Test Station China Lake, California Attn: Head, Chemistry Division (1)

Technical Report Distribution List

Page 2

<p>Commanding Officer Army Research Office Box CM, Duke Station Durham, North Carolina Attn: Scientific Synthesis Office (1)</p>	<p>Inspector of Naval Material 495 Summer Street Boston 10, Massachusetts (1)</p>
<p>Brookhaven National Laboratory Chemistry Department Upton, New York (1)</p>	<p>Mr. R. A. Osteryoung Atomics International Canuga Park, California (1)</p>
<p>Atomic Energy Commission Division of Research Chemistry Programs Washington 25, D. C. (1)</p>	<p>Dr. David M. Mason Stanford University Stanford, California (1)</p>
<p>Atomic Energy Commission Division of Technical Information Extension Post Office Box 62 Oak Ridge, Tennessee (1)</p>	<p>Dr. Howard L. Recht Astropower, Inc. 2968 Randolph Avenue Costa Mesa, California (1)</p>
<p>U. S. Army Chemical Research and Development Laboratories Technical Library Army Chemical Center, Maryland (1)</p>	<p>Mr. L. R. Griffith California Research Corporation 576 Standard Avenue Richmond, California (1)</p>
<p>Office of Technical Services Department of Commerce Washington 25, D. C. (1)</p>	<p>Dr. Ralph G. Gentile Monsanto Research Corporation Boston Laboratories Everett 49, Massachusetts (1)</p>
<p>Commanding Officer Office of Naval Research Branch Office 495 Summer Street Boston 10, Massachusetts (1)</p>	<p>Dr. Ray M. Hurd Texas Research Associates 1701 Guadalupe Street Austin 1, Texas (1)</p>
<p>Director, ARPA Attn: Dr. j. H. Huth Material Sciences Room 3D155 The Pentagon Washington 25, D. C. (4)</p>	<p>Dr. C. E. Heath Esso Research & Engineering Company Box 51 Linden, New Jersey (1)</p>
<p>Dr. S. Schuldiner Naval Research Laboratory Code 6160 Washington 25. D. C. (1)</p>	<p>Dr. Richard H. Leet American Oil Company Whiting Laboratories Post Office Box 431 Whiting, Indiana (1)</p>
<p>Dr. R. F. Baddour Department of Chemistry Mass. Institute of Technology Cambridge 39, Massachusetts (1)</p>	<p>Dr. G. C. Szego Institute for Defense Analysis 1666 Connecticut Avenue N. W. Washington 9, D. C. (1)</p>

Dr. Douglas W. McKee General Electric Company Research Laboratories Schenectady, New York	(1)	Dr. T. P. Dirkse Department of Chemistry Calvin College Grand Rapids, Michigan	(1)
Dr. E. A. Oster General Electric Company, DECO Lynn, Massachusetts	(1)	Dr. George J. Janz Department of Chemistry Rensselaer Polytechnic Institute Troy, New York	(1)
Dr. R. R. Heikes Solid State Phenomena Department Westinghouse Electric Corporation Pittsburgh, Pennsylvania		Mr. N. F. Blackburn E. R. D. L. Materials Branch Fort Belvoir, Virginia	(1)
Prof. Herman P. Meissner Massachusetts Institute of Technology Cambridge 39, Massachusetts	(1)	Dr. G. Barth-Wehrenalp, Director Inorganic Research Department Pennsalt Chemicals Corporation Box 4388 Philadelphia 18, Pennsylvania	(2)
Mr. Donald P. Snowden General Atomic Post Office Box 608 San Diego 12, California	(1)	Dr. B. R. Sundheim Department of Chemistry New York University New York 3, New York	(1)
Prof. C. Tobias Chemistry Department University of California Berkeley, California	(1)	Dr. B. R. Stein European Research Office U. S. Army R&D Liaison Group 985 IDU APO 757, New York, N. Y.	(1)
Dr. Y. L. Sandler Westinghouse Research Laboratories Schenectady, New York	(1)	Dr. E. M. Cohn NASA Code RPP 1512 H Street N. W. Washington 25, D. C.	(1)
Dr. Paul Delahay Department of Chemistry Louisiana State University Baton Rouge, Louisiana	(1)	Dr. E. Yeager Department of Chemistry Western Reserve University Cleveland 6, Ohio	(1)
Dr. W. J. Hamer Electrochemistry Section National Science Foundation Washington 25, D. C.	(1)	Lockheed Aircraft Corporation Missiles and Space Division Technical Information Center 3251 Hanover Street Palo Alto, California	(1)
Dr. Herbert Hunger Power Sources Division U. S. Army Signal Research & Development Laboratory Fort Monmouth, New Jersey			